Some aspects of the photochemistry of fullerenes

Alguns aspectos da fotoquímica dos fulerenos

MÁRIO N. BERBERAN E SANTOS

CENTRO DE QUÍMICA-FÍSICA MOLECULAR, INSTITUTO SUPERIOR TÉCNICO, 1096 LISBOA CODEX, PORTUGAL

After a short overview of the fullerenes, the more physical aspects of their photochemistry are reviewed, with special emphasis on the polarization of the fluorescence of C_{60} and C_{70}, and on the delayed fluorescence of C_{70}.

Após uma breve panorâmica da origem e presente estado dos conhecimentos sobre os fulerenos, são apresentados alguns aspectos da sua fotoquímica, com particular relevo para a polarização de fluorescência do C_{60} e do C_{70}, e para a fluorescência retardada deste último.

1. Introduction

The discovery of the fullerenes in 1985 by Kroto *et al.* [1] immediately arose great interest. However, it was only after their bulk synthesis in 1990 by Krätschmer *et al.* [2, 3] and almost simultaneously by Taylor *et al.* [4], that the proposed molecular structures were conclusively shown to be correct. It was also only then that the study of the physical and chemical properties of fullerenes became possible. In this work, and after a short overview, the physical aspects of the photochemistry of the fullerenes will be reviewed, with special emphasis on the work carried out at Centro de Química-Física Molecular, IST.

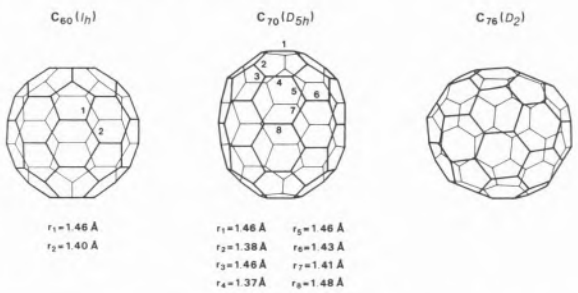

Figure 1 – The structures of C_{60}, C_{70} and C_{76}. For comparison, typical carbon-carbon bond length values are: 1.33 Å in ethene (double bond), 1.40 Å in benzene (aromatic), and 1.54 Å in alkanes (single bond); In naphthalene (see Fig. 2) carbon-carbon bond lengths take values between 1.37 Å and 1.42 Å. Of the two possible IPR isomers of C_{76}, only the one shown has been isolated. It is optically active, with two enantiomeric forms.

Fullerenes are clusters composed by an even number of trivalent (three σ bonds and one π bond) carbon atoms. They have polyhedral shape, with pentagonal and hexagonal faces. The three smallest stable fullerenes are C_{60}, C_{70} and C_{76} (Fig.1). A large number of higher fullerenes was also isolated and characterised, namely C_{78}, C_{82}, C_{84} [5 and references therein] and, more recently, from C_{86} to C_{104}, and even C_{120} [6,7]. Still higher ones, up to C_{460}, have been observed in mass spectra. Much larger fullerene-like structures, either multi- or single-walled, e.g. nanotubes, have also been produced and are the subject of active research, see e.g. [8,9]. Since 1990, many fullerene derivatives, mainly of C_{60} and, to a minor extent, of C_{70}, have been synthesised [10]. They belong to several classes [10b]: (i) exohedral derivatives, like adducts and salts of fullerides, (ii) endohedral complexes, like He@C_{60} and Sc_4@C_{82} (iii) heterofullerenes, like $C_{69}N$ (iv) open cluster compounds, and (v) degradation products. It is interesting to note that the total synthesis of fullerenes remains a challenge for chemists [11].

Among the various clusters originally observed in the mass spectra of laser ablated graphite (C_n, with n = 24, 28, 32, 38, 40, 42, 44, 50, 60,...) only the heavier ones correspond to the stable species present in soot (either prepared by the Krätschmer-Huffman method [2, 3] or simply from hydrocarbon combustion [12]) that have been isolated and characterised (C_n, with n = 60, 70, 76, 78,....). The structure and stability of such clusters can be partially explained on the basis of two simple rules [5, 13a]: (i) in order to reduce angular strain, only pentagonal and hexagonal rings are allowed, and (ii) in order not to reduce the π-energy stabilisation, and simul-

taneously to reduce angular strain, pentagons must be surrounded by hexagons (the so-called isolated pentagon rule, or IPR). Fulfilment of the first rule, together with the celebrated Euler theorem, imply that clusters must have an even number n of atoms and exactly 12 pentagons and $(n\text{-}20)/2$ hexagons [5,13a]. C_{20}, composed exclusively by pentagons, is therefore the first possible fullerene cluster. However, the smallest n for which the IPR is obeyed is 60, the next value being 70 [13]. This justifies why C_{60} and C_{70} are especially abundant in the vapour and are the smallest fullerenes to have been isolated. Above 70, all even n are allowed by the same rules, and above 74, several IPR isomers exist. However, the number of observed isomers is in general much smaller than the maximum possible. For instance, C_{72} and C_{74} are not observed, and of the 35 IPR isomers of C_{88}, only 2 are known. It is suggested that this is due to finer aspects of relative stability and to the formation mechanism of the fullerenes [6]. For very large structures, the possibility of occurrence of heptagons and additional pentagons (usually associated, the so-called azulene or 5/7 defects) also exists [8].

In C_{60} (symmetry point group I_h), all carbon atoms are equivalent, but there are two different bond lengths (Fig. 1). In C_{70} (symmetry point group D_{5h}), there are five classes of carbon atoms, and eight different bond lengths (Fig. 1). In C_{76} (symmetry point group D_2), there are 19 classes of carbon atoms, and 30 different bonds (Fig. 1).

In fullerenes, π-electrons are fairly delocalized, and a simple quantum [14] (or even classical [15]) picture of full delocalization over a sphere is able to explain the gross features of the electronic absorption and dispersion spectra of C_{60}. Nevertheless, as show by the observed diversity of bond lengths, some single-double bond alternancy is retained (Fig. 1), and this has important consequences in the reactivity and regiochemistry of these molecules [10].

2. General aspects of the photochemistry of fullerenes

Our discussion of fullerenes will be mostly devoted to C_{60} and C_{70}. While some of the general conclusions probably apply to other members of the family, photophysical and photochemical informations on the higher fullerenes are scarce. In fact, little more is known than their electronic absorption spectra [4, 6, 7, 16]. This situation will undoubtedly change in the near future.

Absorption and emission

The photophysical properties of these all-carbon molecules result from: (i) Delocalization of π-electrons, (ii) large number of π-electrons and, (iii) high molecular symmetry. The delocalization of the π-electrons over a relatively large surface produces electronic absorption spectra covering most of the visible region, with onsets in the red (C_{60}, C_{70}) or in the near infrared (C_{76}, C_{78}, ...). The fluorescence, with negligible Stokes shift, appears therefore in the red and infrared (C_{60}, C_{70}), while for the higher fullerenes (C_{76}, C_{78}, ...) it is expected to be located in the infrared. Also as a consequence of extended delocalization and large molecular size, the singlet-triplet splitting is small [17,18], and phosphorescence also appears in the extreme red and infrared for C_{60} and C_{70}. The large number of π-electrons (60, 70,...) implies a large density of electronically excited states (Fig. 2), leading to a continuous absorption in the UV and visible, and also to facilitated nonradiative transitions.

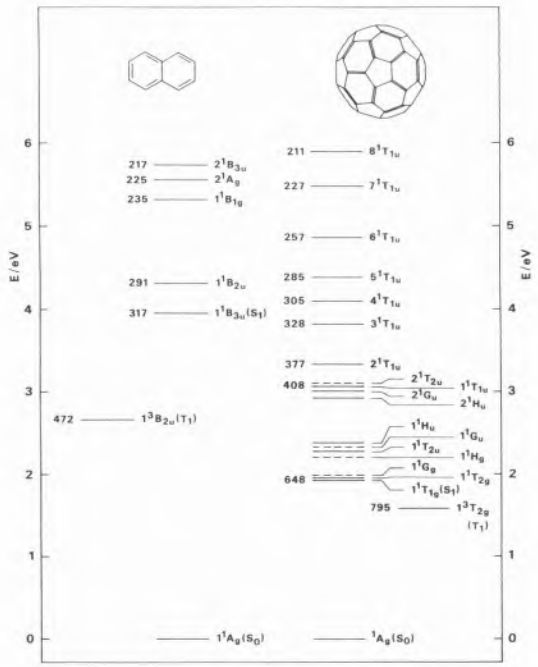

Figure 2. Comparison of the electronic state diagrams of naphthalene (10 π-electrons) and C_{60} (60 π-electrons). The approximate wavelengths (in nm) of the pure electronic transitions are shown on the left. For both molecules, only the first triplet (T_1) is shown. For C_{60}, only the T_{1u} states are shown for energies above 3.3 eV. Note the much higher density of states of C_{60}, as well as the much smaller singlet-triplet gap of this compound. The ionization energies of naphthalene and C_{60} are, respectively, 8.1 eV and 7.6 eV.

Finally, the high molecular symmetry restricts the number of allowed electronic transitions, rendering for example forbidden the S_1-S_0 radiative transition. In this way, the absorption spectra of both C_{60} and C_{70} show weak bands in the visible ($\lambda_{max} \simeq 540$ nm, $\varepsilon_{max} \simeq 710$ $M^{-1}cm^{-1}$, for C_{60}, and $\lambda_{max} \simeq 470$ nm, $\varepsilon_{max} \simeq 14500$ $M^{-1}cm^{-1}$ for C_{70}) but more intense ones in the violet and UV ($\varepsilon_{max} \simeq 10^5$ $M^{-1}cm^{-1}$) [2, 19-21]. Their solutions display a wide variety of beautiful colours, ranging from the "exquisitely delicate magenta" [22] of C_{60}, to the orange-red of C_{70}, and to the bright yellow-green of C_{76} [16]. A thorough study of the colours of C_{60} solutions is given in

[23]. The high molecular symmetry is also responsible for a Jahn-Teller distortion in the emissive (S_1 and T_1) states, for intrinsically low values of the polarization of the luminescence (C_{60}, C_{70}), and for a relatively large spin-orbit coupling [24].

Excited state dynamics

For a discussion of the excited state dynamics of the fullerenes, we refer to the so-called Jablonski diagram, Figure 3. Some important photophysical parameters are given in Table 1. Owing to the small singlet-triplet gap, and to the forbidden nature of the radiative $S_1 \rightarrow S_0$ process (fluorescence), the dominant S_1 decay process for C_{60} and C_{70} (and, in all likeliness, for at least the most symmetric higher fullerenes) is the $S_1 \rightarrow T_1$ intersystem crossing [17, 18]. Indeed, the quantum yield of triplet formation is almost unity in both cases. The fluorescence lifetime is quite short for both molecules, and is almost equal to the inverse of the $S_1 \rightarrow T_1$ intersystem crossing rate constant. This process is much faster than in typical aromatic hydrocarbons. Because it is not activated, the lifetimes and quantum yields are insensitive to temperature. Consistent with the forbidden nature of the radiative process, the fluorescence radiative lifetimes are of the order of 1 microsecond, that is, 3-4 orders of magnitude higher than the actual lifetimes. The quantum yields of fluorescence are therefore small. However, as will be discussed below, in certain favourable conditions, the effective fluorescence quantum yield of C_{70} may increase 10 to 100-fold as a consequence of the $S_1 \rightarrow T_1$ back-intersystem crossing [25]. The phosphorescence of C_{60} has been only studied at or below 77 K [26-28]. Given the variation with temperature observed in C_{70} [25], we regard as provisional the respective values given in Table 1.

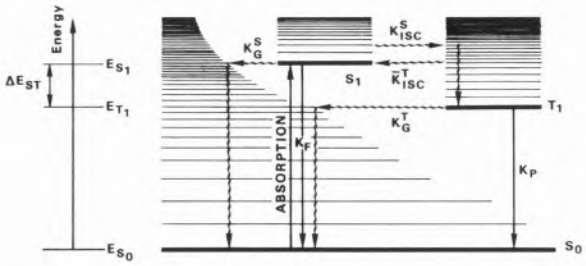

Figure 3. Simplified diagram of the electronic states and kinetic elementary steps after photon absorption (Jablonski diagram). As usual, the radiative processes ($S_1 \leftarrow S_0$ absorption, $S_1 \rightarrow S_0$ fluorescence and $T_1 \rightarrow S_0$ phosphorescence) are represented by straight lines, while the nonradiative processes ($S_1 \rightarrow S_0$ internal conversion, $S_1 \rightarrow T_1$ intersystem crossing, $S_1 \leftarrow T_1$ intersystem crossing, and $T_1 \leftarrow S_0$ intersystem crossing) are represented by wavy lines. It is possible that one or more higher triplets (T_2, etc.) also lie below S_1, thus participating, as intermediates, in the intersystem crossing process.

Table 1. Some photophysical parameters of C_{60} and C_{70}

	C_{60}	C_{70}
$\lambda(S_1\text{-}S_0)$ / nm	648	650
$\lambda(T_1\text{-}S_0)$ / nm	795	750
ΔE_{ST} / kJ mol^{-1}	34	25
τ_F / ns	1.1	0.65
τ_R / μs	2-6	1
Φ_F	2×10^{-4}	5×10^{-4}
Φ_T	≃1	0.994
τ_P / ms	0.4	50
Φ_P	n.a.	10^{-3}
S_Δ	≃1.0	≃0.9

Singlet oxygen

One of the interesting aspects of both C_{60} and C_{70} is their ability to produce singlet oxygen O_2 ($^1\Delta_g$) with almost unit efficiency, $S_\Delta \simeq 1$ [17, 18, 29]. On the one hand, their quantum yield of triplet formation is close to unity, and the quenching of the fullerene triplet by oxygen through triplet-triplet annihilation, is close to

$$^3C_n^* + {}^3O_2 \rightarrow {}^1C_n + {}^1O_2^* \quad (n = 60, 70) \qquad (1)$$

diffusion control. On the other hand, the reverse process (i.e., quenching of singlet oxygen by ground state fullerenes) proceeds at a rate much smaller than diffusion control [17, 30]. This fact, together with the low fluorescence quantum yield, makes the fullerenes very good photosensitizers [31].

Optical limiting behaviour

Within a certain wavelength range, fullerenes present the interesting property of an effective absorption coefficient that increases with the incident light intensity [32, 33]. In this way, solutions or films of these compounds respond nonlinearly to the incident light, being more opaque to the higher intensities. This appears to occur in those spectral regions where the triplet-triplet intrinsic absorption coefficients are considerably higher than the corresponding singlet-singlet ones, mainly on account of an increasing population of the triplet state with intensity (reverse saturable absorption, or RSA). Both the incident pulse duration and repetition rate play an important role, because the T_1 population evolution depends on the interplay of external excitation and internal photophysical kinetics. Simplified kinetic models for RSA exist [34, 35]. The physical picture is complicated by the possibility of alternative or at least co-existing mechanisms, namely thermal lensing and

nonlinear light scattering [33, 36]. Considerable effort towards applications is well underway [37].

3. Fluorescence polarization of C_{60} and C_{70}

The linear polarization of the fluorescence emitted at a right angle with the excitation direction is conveniently measured by the quantity anisotropy, r [38],where

$$r = \frac{I_{||} - I_{\perp}}{I_{||} + 2I_{\perp}} \qquad (2)$$

$I_{||}$ is the intensity of the fluorescence with vertical polarization and I is the intensity of the fluorescence with horizontal polarization, the excitation being made with vertically polarized light (Fig. 4). For a ground state isotropic distribution of molecules, the fluorescence

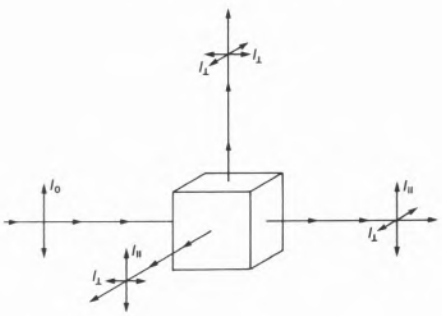

Figure 4. Isotropic sample excited with vertically polarized light. The fluorescence emitted in the plane perpendicular to the polarisation direction of the excitation may be decomposed in vertically polarized (parallel, $I_{||}$) and horizontally polarized (perpendicular, $I_{\perp}$) components.

anisotropy is a direct measure of the angular correlation between the (one-photon) absorption and the emission transition dipoles [39]

$$r(t) = 0.4 \frac{3 < \cos^2 \alpha > (t) - 1}{2} \qquad (3)$$

where α is the angle between absorption and emission transition dipoles and <···> denotes the ensemble average which is in general a function of time.

If rotation and energy migration do not occur within the excited state lifetime, the anisotropy in response to excitation by a $\delta(t)$ pulse is constant in time and identical to that obtained for steady-state excitation. In such a case, both reduce to the fundamental anisotropy r_o [39], where <...> is now an average over the

$$r_o = 0.4 \frac{3 < \cos^2 \alpha > - 1}{2} \qquad (4)$$

angular distribution within the molecular framework. Upper and lower bounds for the fundamental anisotropy are 0.4 (collinear absorption and emission) and -0.2 (orthogonal absorption and emission).

If three mutually perpendicular axes are defined with respect to the molecular framework (molecular frame), these three axes are frequently non-equivalent from the symmetry point of view. In that case, the angle α is unique for a given pair of excitation and emission wavelengths; In particular it is zero for excitation at the 0-0 band of S_1, provided the emitting S_1 retains the Franck-Condon geometry. Hence, the fundamental anisotropy takes its maximum value, 0.4, when exciting at the S_1 0-0 band.

However, if two of the axes of the molecular frame are equivalent, *x* and *y* say, and if the absorption and the (several equivalent) emission transition moments occur in the *xy* plane, then the fundamental anisotropy will have as a maximum value only 0.1 [40, 41]. This was conclusively shown to be the case for benzene (ground state symmetry point group D_{6h}) and triphenylene (ground state point group D_{3h}) [40-42].

For the even more symmetrical molecules belonging to the tetrahedral, octahedral and icosahedral point groups, where the *x*, *y* and *z* axes are equivalent, the possibility of intrinsically unpolarized fluorescence arises.

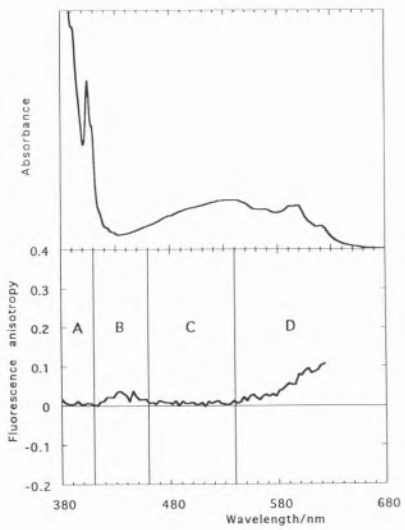

Figure 5. Electronic absorption spectrum (top) and excitation polarization (bottom) of 2×10^{-4} M C_{60} in toluene-ethanol (10:1) glass at 140 K. Owing to weakness of the fluorescence, the measured anisotropy departs from zero in regions B and D, where stray light (B, D) and polarized Raman scattering from toluene (D) have comparable intensity [50].

An interesting candidate would be the C_{60} molecule, that belongs to the icosahedral (I_h) point group, as convincingly shown by its ^{13}C-NMR [4, 43], IR absorption [3, 44], and vibrational Raman [44] spectra. The discovery of C_{60} weak fluorescence [45-48], prompted us to investigate its fundamental polarization, predicted some years before to be nil [49]. It was indeed found that the fluorescence of C_{60} had negligible polarization when measured in low temperature, optically transparent rigid organic glasses (Figures 5, 6 and 7) [50, 51]. It was thus concluded that the fluorescence is intrinsically unpolarized, as expected on theoretical grounds. C_{60} is probably the first molecule to display intrinsically unpolarized fluorescence.

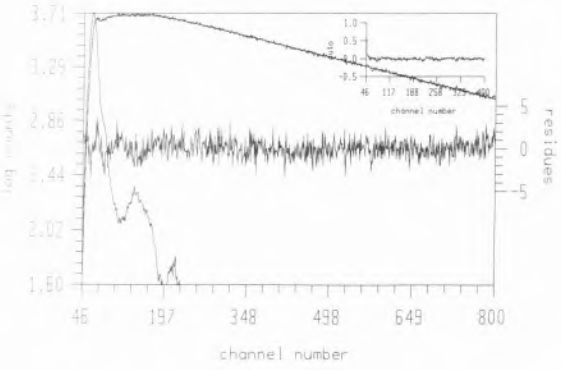

Figure 6. Fluorescence decay of C_{60} in a methylcyclohexane-toluene (7:2) glass at 110 K, obtained with the picosecond laser system of CQFM [51]. $[C_{60}] = 8 \times 10^{-5}$ M. Excitation and emission wavelengths were 595 nm and 690 nm. The time scale was 2.77 ps/channel. The Raman scattering can be seen as a first peak in the decay (the possibility that it was due to excitation scattered light is ruled out by its emission wavelength dependence and because a cut-off filter was used). The decay is well fitted (reduced chi-squared = 1.21, random residuals and negligible autocorrelation) by a sum of three exponentials, one of which, of zero lifetime, accounts for the Raman scattering, the other two having τ_1 = 1.09 ns (α_1 = 1.25) and τ_2 = 0.10 ns (α_2 = -0.25). The 100 ps component is only observed at low temperature.

From the point of view of symmetry, C_{70} is again an interesting molecule. The molecule is known to belong to the D_{5h} point group, thus having two equivalent axes (*x* and *y*). The electronic transition moment for S_1–S_0 may in principle occur either along the *z*-axis or in the *xy*-plane. In the first case, the fundamental anisotropy of C_{70} may take values between 0.4 and -0.2, depending on the excitation wavelength. In the second case, the fundamental anisotropy of C_{70} may take values only between 0.1 and -0.2, depending on the excitation wavelength. As mentioned above, cases where 0.1 is the maximum allowed value are known for planar molecules belonging to the D_{nh} point groups ($n \geq 3$). In these, however, anisotropy values cannot be different from 0.1, because all singlet-singlet one-photon transitions are in-

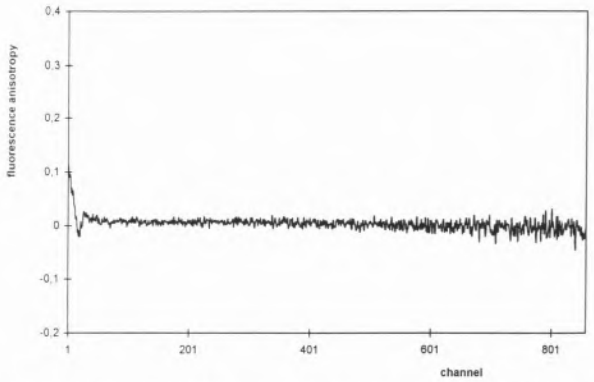

Figure 7. Experimental fluorescence anisotropy decay of C_{60} in a methylcyclohexane-toluene (7:2) glass at 110 K, obtained with the picosecond laser system of CQFM [51]. $[C_{60}] = 8 \times 10^{-5}$ M. Excitation and emission wavelengths were 595 nm and 690 nm. The time scale was 2.77 ps/channel. It is seen that, after the impulse duration (FWHM = 35 ps, or 13 channels), the anisotropy has a nearly constant value very close to zero (0.001 ± 0.005). Note that the Raman scattering, being much faster than fluorescence, does not affect the results, that fall into region D of the steady-state experiment (Fig. 5).

plane, whereas in C_{70} out-of-plane ones (i.e. along the z-axis) are also possible. The only available theoretical calculation on the polarization of the electronic transitions of C_{70} [52], predicts the electronic transition moment for $S_1 \leftarrow S_0$ to be in the *xy*-plane. Our experimental results [51] support such a conclusion (Fig. 8): The anisotropy is never above 0.1, even when close to the

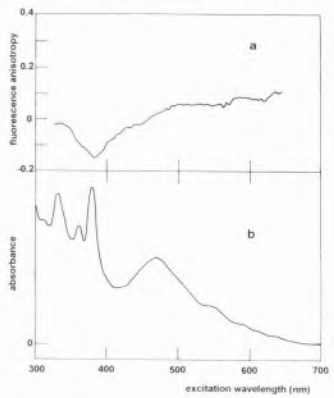

Figure 8. (a) Steady-state anisotropy of C_{70} in a methylcyclohexane-toluene (7:2) glass at 110 K, and, (b) Absorption spectrum of C_{70} a methylcyclohexane-toluene (7:2) glass at room temperature, both as a function of the excitation wavelength. $[C_{70}] = 7 \times 10^{-5}$ M. The small oscillations observed in (a) are due to noise.

absorption on-set. The first electronic transition of C_{70} is thus polarized in the *xy* plane, in agreement with the calculations by the tight-binding model [52]. It can also be seen in Fig. 8 that the anisotropy attains a minimum at ca. 380 nm. This minimum, close to -0.2, coincides with the peak wavelength (378 nm) of a strong absorption band that is therefore *z*-polarized.

4. Delayed fluorescence of C_{70}

Molecular fluorescence is almost always the result of a two-step process: a transition from the ground state to an electronically excited state (absorption) followed by a transition from the same excited state (or another one of lower energy, after fast relaxation) to the ground state (*prompt fluorescence*, PF), see Figure 3. For the common case of closed-shell molecules, the states involved in the last step are S_0 (ground singlet state) and usually S_1 (first excited singlet). However, fluorescence can also occur by a more complicated route, *via* the triplet manifold: after excitation, and once attained S_1, there is an intersystem crossing to the triplet manifold (triplet state T_1), and then, after vibrational thermalization, a second intersystem crossing back to S_1, followed by emission proper (Figure 3). This second type of fluorescence, called *thermally activated delayed fluorescence* (TDF), is significant only if the two following conditions are met: (i) reasonably high probability of $S_1 \rightarrow T_1$ intersystem crossing, i.e., high quantum yield of triplet formation Φ_T where

$$\Phi_T = \frac{k^S_{ISC}}{k_F + k^S_G + k^S_{ISC}} \qquad (5)$$

and, (ii) reasonably high probability ofsubsequent $S_1 \leftarrow T_1$ back intersystem crossing, i.e., high quantum yield of singlet formation, Φ_S, which by analogy with Eq. 5 is defined

$$\Phi_S = \frac{k^T_{ISC}}{k_p + k^T_G + k^T_{ISC}} \qquad (6)$$

In fact, it follows from the kinetic model depicted in Figure 3 that the steady-state intensities ratio of delayed fluorescence (DF) to prompt fluorescence (PF) is given by

$$\frac{I_{DF}}{I_{PF}} = \frac{\Phi_{DF}}{\Phi_{PF}} = \frac{1}{\frac{1}{\Phi_S \Phi_T} - 1} \qquad (7)$$

From the theory of nonradiative transitions, it is known that high values of k^S_{ISC} are favoured by a small ΔE_{ST} (S_1 - T_1 gap). The same holds *a fortiori* for k^T_{ISC}, because it is *approximately* given by [53, 54]

$$k^T_{ISC} = \overline{k}^T_{ISC} \exp\left(-\frac{\Delta E_{ST}}{RT}\right) \qquad (8)$$

where $\overline{k}^T_{ISC}$ is the average rate constant for the adiabatic $S_1 \rightarrow T_1$ intersystem crossing, and the exponential factor is the fraction of triplets whose total internal energy (electronic + vibrational) is equal or larger than the electronic energy of S_1. Therefore, TDF is only possible for molecules with small ΔE_{ST} and even then at not too low temperatures.

Although known for many years [53 and references therein], the phenomenon of TDF remains extremely rare. In most of the cases studied, including the classic one, eosin [53], it is exceedingly weak, in the sense that $\Phi_{DF} << \Phi_{PF}$.

The known photophysical properties of C_{70}, namely the quantum yield of triplet formation close to one [18, 29, 55, 56], the small S_1 - T_1 gap [18, 27, 57, 58] and the long intrinsic phosphorescence lifetime [57-60], all favour TDF for this molecule.

In fact, we have observed exceptionally *strong* TDF ($\Phi_{DF} >> \Phi_{PF}$) for C_{70} dissolved in degassed liquid and solid paraffin [25]. The same study disclosed an intriguing variation of the phosphorescence spectrum with temperature, and enabled the revision of the published values of ΔE_{ST} and of Φ_T, the last one obtained with unprecedented precision from a new kinetic analysis.

The luminescence spectrum of C_{70} in paraffin is shown in Figure 9. It consists of a high energy system, fluorescence (630 nm - 750 nm), and a low energy system, phosphorescence (>750 nm). A Parker plot (i.e., $\ln(I_{DF} / I_P)$ vs. 1/T, where I_P is the phosphorescence intensity) of 10^{-5} M degassed solutions of C_{70} , from -59°C to 5°C, gives a straight line, from whose slope one obtains ΔE_{ST} = 26 ±1 kJ/mol. On the other hand, for degassed solutions and temperatures above -20°C, DF is much stronger than PF (Figure 10; at the highest recorded temperature, 70°C, it is 50 times stronger). Using the new method of analysis described in [25], for temperatures from -20°C to 70°C, one obtains a singlet-triplet gap of

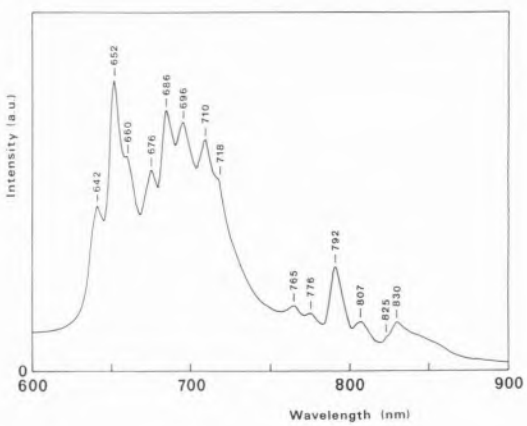

Figure 9. Luminescence spectrum of C_{70} dissolved in paraffin, at -30 °C. $[C_{70}] = 2.5 \times 10^{-5}$ M. Excitation and emission slits were 18 nm and 2 nm, respectively. The fluorescence spans the range 630 nm - 750 nm. The fluorescence band at 642 nm appears to be a hot band. The phosphorescence begins at ca. 750 nm, and extends further to the infrared (not shown).

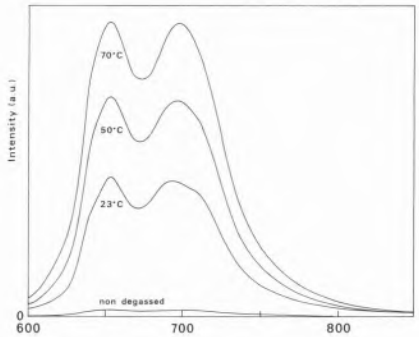

Figure 10. Low resolution fluorescence spectra of a 1.4×10^{-6} M solution of C_{70} in liquid paraffin. Degassed solution at 23 °C, 50 °C, and 70 °C. The intensity of the non degassed solution is independent of temperature, and is entirely due to prompt fluorescence. The rise with temperature observed in the degassed solutions results from the increasing contribution of delayed fluorescence to the total intensity. Emission slits were 9 nm.

25 ±1 kJ/mol, in good agreement with the value recovered from the Parker plot. From the accepted spectroscopic assignment of 652 nm as the 0-0 band of the fluorescence [58, 61], the determined range of values of ΔE_{ST} (24 kJ/mol - 27 kJ/mol) places the 0-0 band of the phosphorescence in the range 750 nm - 765 nm. The phosphorescence spectrum recorded at -85 °C, where delayed fluorescence is negligible, has indeed its on-set at ca. 750 nm (Fig. 11). Careful examination of the

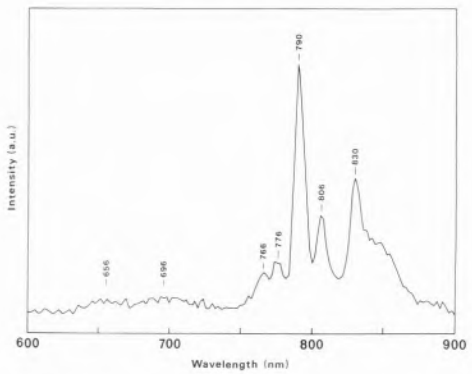

Figure 11. Phosphorescence spectrum of C_{70} in solid paraffin at -85°C. The residual delayed fluorescence is seen as two very weak bands on the left. Time delay: 10 ms.

room temperature luminescence spectrum of a degassed solution (dominated by delayed fluorescence, Fig. 12) shows again a weak shoulder at 776 nm and weak bands at 791 nm and 830 nm, making very likely that the phosphorescence spectrum does not change significantly for temperatures higher than at least -85 °C. Previous studies of the phosphorescence spectrum [26, 27, 46, 57, 58] have not explored the temperature region above 77 K and, as a consequence, the high energy bands were not observed. This occurs because on cooling down to ca. 77 K or less, and thus well below the temperature region where significant TDF is obser-

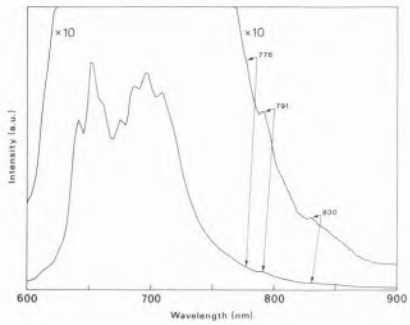

Figure 12. Luminescence of a 10^{-5} M degassed solution of C_{70} in liquid paraffin, at room temperature. The phosphorescence barely emerges from the fluorescence tail.

ved, the high energy system of bands looses intensity, and the first noticeable band of the phosphorescence spectrum appears at 788 nm (77 K), or even at 806 nm (methylcyclohexane at 10 K) [58]. This peculiar behaviour could be due to solid matrix effects [10].

The data analysis performed according to the new method also yields $\bar{k}^{T}_{ISC} \simeq 10^{7}\ s^{-1}$. This value is to be compared with that of the direct intersystem crossing, $k^{S}_{ISC} = 2 \times 10^{9}\ s^{-1}$, which is simply computed as the inverse of the fluorescence lifetime (ca. 650 ps). The difference between the two rate constants does not appear unreasonable, in view of the much higher density of final states expected for the direct intersystem crossing case.

A quantum yield of triplet formation $\Phi_T = 0.994 \pm 0.001$, is also obtained. This value is to be compared with the published ones, obtained by more sophisticated techniques [18, 29, 55, 56], 0.76 ± 0.15, 0.97 ± 0.03, 1 ± 0.15, and 0.90 ± 0.15, and is believed to be substantially more accurate, especially as a lower bound. Using the determined value of Φ_T and Eq. 7, one obtains for the high temperature limit ($\Phi_S = 1$), that $\left(\frac{I_{DF}}{I_{PF}}\right)_{max} = 166$. In this way, the global fluorescence quantum yield ($\Phi_F = \Phi_{PF} + \Phi_{DF}$) of C_{70} can in principle be 167 times higher than that of prompt fluorescence, and thus attain the very respectable value of $167 \times 5 \times 10^{-4} = 0.08$.

5. Concluding remarks

The chemistry and photochemistry of fullerenes and derivatives is an area in great expansion, and with almost unlimited possibilities, given the diversity of structures covered. As regards applications, it also offers great promise.

Acknowledgements

The work described in the last two sections was done in collaboration with Professor Bernard Valeur

(CNAM, Paris, and ENS Cachan), Ing. Jean-Pierre Lefèvre (CNAM, Paris, and ENS Cachan), Dr. Aleksandre Fedorov (CQFM, IST) and Eng. João M.M. Garcia (CQFM, IST).

References

1. H.W. Kroto, J.R. Heath, S.C. O'Brien, R.F. Curl, R.E. Smalley, *Nature* **318** (1985) 162.
2. W. Krätschmer, K. Fostiropoulos, D.R. Huffman, *Chem. Phys. Letters* **170** (1990) 167.
3. W. Krätschmer, L.D. Lamb, K. Fostiropoulos, D.R. Huffman, *Nature* **347** (1990) 354.
4. R. Taylor, J.P. Hare, A.K. Abdul-Sada, H.W. Kroto, *J. Chem. Soc. Chem. Commun.* (1990) 1423.
5. J. Cioslowski, *Electronic Structure Calculations on Fullerenes and Their Derivatives*, Oxford University Press, New York and Oxford, 1995.
6. Y. Achiba, Proceedings of Fullerenes '96, to be published in *J. Phys. Chem. of Solids*.
7. H. Richter, K. Taghizadeh, W.J. Grieco, A.L. Lafleur, J.B. Howard, Proceedings of Fullerenes '96, to be published in *J. Phys. Chem. of Solids*.
8. T.W. Ebbesen, *Phys. Today*, June 1996, 26.
9. A. Thess, R. Lee, P. Nikolaev, H. Dai, P. Petit, J. Robert, C. Xu, Y.H. Lee, S.G. Kim, A.G. Rinzler, D.T. Colbert, G.E. Scuseria, D. Tománek, J.E. Fischer, R.E. Smalley, *Science* **273** (1996) 483.
10. (a) R. Taylor, D.R.M. Walton, *Nature* **363** (1993) 685. (b) A. Hirsch, Proceedings of Fullerenes '96, to be published in *J. Phys. Chem. of Solids*.
11. P.W. Rabideau, A. Sygula, *Acc. Chem. Res.* **29** (1996) 235.
12. J.B. Howard, J.T. McKinnon, Y. Makarovsky, A.L. Lafleur, M.E. Johnson, *Nature* **352** (1991) 139.
13. (a) H. W. Kroto, *Nature* **329** (1987) 529. (b) T.G. Schmalz, W.A. Seitz, D.J. Klein, G.E. Hite, *J. Am. Chem. Soc.* **110** (1988) 1113.
14. (a) M. R. Savina, L.L. Lohr, A.H. Francis, *Chem. Phys Letters* **205** (1993) 200. (b) M. N. Berberan-Santos, *Quím. Nova* **17** (1994) 293.
15. D. Östling, A. Rosén, P. Apell, G. Mukhopadhyay, *Proc. SPIE* **2284** (1994) 48.
16. (a) F. Diederich, R.L. Whetten, *Acc. Chem. Res.* **25** (1992) 119. (b) K. Kikuchi, N. Nakahara, T. Wakabayashi, M. Honda, H. Matsumiya, T. Moriwaki, S. Suzuki, H. Shiromaru, K. Saito, K. Yamauchi, I. Ikemoto, Y. Achiba, *Chem. Phys. Letters* **188** (1992) 177.
17. J. W. Arbogast, A. O. Darmanyan, C. S. Foote, Y. Rubin, F. N. Diederich, M. M. Alvarez, S. J. Anz and R. L. Whetten, *J. Phys. Chem.* **95** (1991) 11.
18. J. W. Arbogast and C. S. Foote, *J. Am. Chem. Soc.* **113** (1991) 8886.
19. H. Ajie, M.M. Alvarez, S.J. Anz, R.D. Beck, F. Diederich, K. Fostiropoulos, D.R. Huffman, W. Krätschmer, Y. Rubin, K.E. Schriver, D. Sensharma, R.L. Whetten, *J. Phys. Chem.* **94** (1990) 8630.
20. J.P. Hare, H.W. Kroto, R. Taylor, *Chem. Phys. Letters* **177** (1991) 394.
21. R.M. Williams, J.W. Verhoeven, *Chem. Phys. Letters* **194** (1992) 446.
22. H.W. Kroto in *The Fullerenes*, H.W. Kroto, J.E. Fischer and D.E. Cox eds., Pergamon, Oxford, 1993.
23. J. Catalán, J.L.Saiz, J.L. Laynez, N. Jagerovic, J. Elguero, *Angew. Chem. Int. Ed. Engl.* **34** (1995) 105.
24. (a) P.M. Allemand, G. Srdanov, A. Koch, K. Khemani, F. Wudl, *J. Am. Chem. Soc.* **113** (1991) 2780. (b) F. J. Adrian, *Chem. Phys.* **211** (1996) 73.
25. M.N. Berberan-Santos, J.M.M. Garcia, *J. Am. Chem. Soc.* **118** (1996) 9391.
26. Y. Zeng, L. Biczok, H. Linschitz, *J. Phys. Chem.* **96** (1992) 5237.
27. K. Palewska, J. Sworakowski, H. Chojnacki, E. C. Meister, U. P. Wild, *J. Phys. Chem.* **97** (1993) 12167.
28. D.J. Heuvel, I.Y. Chan, E.J.J. Groenen, J. Schmidt, G. Meijer, *Chem. Phys. Letters* **231** (1994) 111.
29. R.R. Hung, J.J. Grabowski, *Chem. Phys. Letters* **192** (1992) 249.
30. A.A. Krasnovsky Jr, C.S. Foote, *J. Am. Chem. Soc.* **115** (1993) 6013.
31. M. Selke, C.S. Foote, *J. Am. Chem. Soc.* **115** (1993) 1166.
32. L.W. Tutt, A. Kost, *Nature* **356** (1992) 225.
33. A. Kost, J.E. Jensen, M.B. Klein, J.C. Withers, R.O. Loufty, M.B. Haeri, M.E. Ehritz, *Proc. SPIE* **2284** (1994) 208.
34. F. Henari, J. Callaghan, H. Stiel, W. Blau, D.J. Cardin, *Chem. Phys. Letters* **199** (1992) 144.
35. J.R. Heflin, S. Wang, D. Marciu, C. Figura, R. Yordanov, *Proc. SPIE* **2530** (1995) 176.
36. S.R. Misra, H.S. Rawat, M.P. Joshi, S.C. Mehendale, K.C. Rustagi, *Proc. SPIE* **2284** (1994) 220.
37. R. Signorini, M. Zerbetto, M. Meneghetti, R. Bozio, M. Maggini, C. Favei, M. Prato, G. Scorrano, *J. Chem. Soc. Chem. Commun.* (1996) 1891.
38. A. Jablonski, *Bull. Acad. Polon. Sci., Ser. Math. Astr. Phys.* **8** (1960) 259.
39. (a) F. Perrin, *Ann. Phys. (Paris)*, **12** (1929) 169. (b) A. Jablonski, *Z. Naturforsch.* **16a** (1961) 1.
40. P.P Feofilov, *The Physical Basis of Polarized Emission*, Consultants Bureau, N.Y., 1961.
41. F. Dörr, *Angew. Chem. Int. Ed. Engl.* **5** (1966) 478.
42. R.D. Hall, B. Valeur and G. Weber, *Chem. Phys. Letters* **116** (1985) 202.
43. R.D. Johnson, G. Meijer, D.S. Bethune, *J. Am. Chem. Soc.* **112** (1990) 8983.
44. D.S. Bethune, G. Meijer, W.C. Tang, H.J. Rosen, W.G. Golden, H. Seki, C.A. Brown and M.S. de Vries, *Chem. Phys. Letters* **179** (1991) 181.
45. C. Reber, L. Yee, J. McKiernan, J.I. Zink, R.S. Williams, W.M. Tong, D.A.A. Ohlberg, R.L. Whetten and F. Diederich, *J. Phys. Chem.* **95** (1991) 2127.
46. S.P. Sibley, S.M. Argentine and A.H. Francis, *Chem. Phys. Letters* **188** (1992) 187.
47. Y. Wang, *J. Phys. Chem.* **96** (1992) 764.
48. D. Kim, M. Lee, Y.D. Suh and S.K. Kim, *J. Am. Chem. Soc.* **114** (1992) 4429.
49. M.N. Berberan e Santos, *Polarização da luminescência molecular*, IST, 1987.
50. M.N. Berberan-Santos, B. Valeur, *J. Chem. Soc. Faraday Trans.* **90** (1994) 2623.
51. A. Fedorov, M.N. Berberan-Santos, J.P. Lefèvre, B. Valeur, submitted to *Chem. Phys. Letters*.
52. J. Shumway and S. Satpathy, *Chem. Phys. Letters* **211** (1993) 545.
53. C.A. Parker, *Photoluminescence of Solutions*, Elsevier, Amsterdam, 1968.
54. F. Tanaka, M. Okamoto, S. Hirayama, *J. Phys. Chem.* **99** (1995) 525.
55. D.K. Palit, A.V. Sapre, J.P. Mittal, C.N.R. Rao, *Chem. Phys. Letters* **195** (1992) 1.
56. R.V. Bensasson, T. Hill, C. Lambert, E.J. Sand, S. Leach, T.G. Truscott, *Chem. Phys. Letters* **206** (1993) 197.
57. S.M. Argentine, A.H. Francis, C.-C. Chen, C.M. Lieber, J.S. Siegel, *J. Phys. Chem.* **98** (1994) 7350.
58. S. M. Argentine, K. T. Kotz, A. H. Francis, *J. Am. Chem. Soc.* **117** (1995) 11762.
59. M. R. Wasielewski, M. P. O'Neil, K. R. Lykke, M. J. Pellin, D. M. Gruen, *J. Am. Chem. Soc.* **113** (1991) 2774.
60. H.T. Etheridge, R.B. Weisman, *J. Phys. Chem.* **99** (1995) 2782.
61. Y.-P. Sun, C.E. Bunker, *J. Phys. Chem.* **97** (1993) 6770.